15th Triennial World Congress, Barcelona, Spain

A RIPPLE MINIMIZATION STRATEGY FOR DIRECT TORQUE AND FLUX CONTROL OF INDUCTION MOTORS USING SLIDING MODES

Mónica Romero [*] **Julio H. Braslavsky** [**] **María I. Valla** [***]

[*] *Depto. de Electrónica, Universidad Nacional de Rosario*
Riobamba 245 bis, (2000) Rosario, Argentina
[**] *Depto. de Ciencia y Tecnología, Universidad Nacional de Quilmes*
and CONICET, Calchaquí al 5800, (1888) F. Varela, Argentina
[***] *LEICI, Depto. de Electrotecnia , Universidad Nacional de La Plata*
and CONICET, CC91, (1900) La Plata, Argentina

Abstract: We present a direct torque and flux control (DTFC) design for an electric induction motor using a sliding-mode control technique. A distinctive feature of our approach is that, by appropriately parameterizing and implementing the sliding-mode controller, we explicitely take into account the discontinuous nature of the actuator in the design process. As a result, we obtain an improved implementation of DTFC, which significantly reduces the levels of steady-state ripple with respect to those typically obtained with conventional implementations of DTFC.

Keywords: Torque control, Sliding-mode control, Induction motors, Electrical machines, Steady-state errors.

1. INTRODUCTION

Vector control of electrical drives, with its two main commercial implementation approaches, Field Oriented Control (FOC) and Direct Flux and Torque Control (DTFC), has generated much discussion comparing advantages and disadvantages of each scheme (e.g., Le-Huy, 1995; Vas, 1998). On one hand, FOC appears as having a better performance than DTFC in a wide range of speed and load conditions. However, the performance of a FOC implementation critically depends on very accurate coordinate transformations and flux angle estimation, which are complex. This complexity leads to significantly more computations than those of the simpler alternative of an equivalent DTFC implementation, which normally only requires setting up a *lookup table* that specifies the actuation for each given torque and flux condition.

On the other hand, the simplicity of DTFC contrasts with some performance limitations, which essentially arise from the way the inverter driving the motor operates in this approach. Namely,

(1) The inverter operates at a variable switching frequency, and moreover, there is no control on the number of switches at a given update of the control signal.
(2) The inverter can only generate a restricted set of actuating signals for a range of operating conditions for which the maximum DC bus is always applied, independently of the magnitude of the error signal or the load of the motor.

These characteristics give rise to difficulties in startup (machine magnetization) and increased levels of steady-state torque ripple.

Because the simplicity of DTFC is highly desirable in many applications, a number of recent works have suggested different strategies to circumvent its performance limitations. For example, Kazmierkowki and Kasprowicz (1995) have proposed the introduction of an additional carrier signal to the torque controller

input to improve startup and low speed operation, while Takahashi and Noguchi (1997); Idris and Yatim (2000); J.Kang and Sul (1998) suggest double parallel PWM-Inverter, injection of dither signal, triangular signal, and calculation of optimal switching technique for the reduction of steady-state torque ripple.

In recent works, Yan et al. (2000) and Romero and Valla (2000) have proposed modified DTFC control schemes based on the *sliding-mode* control (SMC) design technique (Utkin, 1993). A distinctive feature of the SMC of electrical drives is that the discontinuous nature of the actuator (the inverter) may be explicitely taken into account within the design process. Moreover, being SMC a Lyapunov-based design technique (Khalil, 1996, §13), it brings in the design process a powerful set of modern nonlinear control tools to further analyze and tune the control system.

In this paper, we propose extensions to the SMC scheme presented in Romero and Valla (2000). Firstly, we propose a methodology to design the inverter DC-bus value to guarantee convergence of the SMC (§3). Secondly, we present two strategies for the implementation of the SMC to achieve a significant reduction of the steady-state torque ripple, in comparison witn those obtained using conventional DTFC schemes (§4). We discuss and compare these results in §5, illustrating the performance of the proposed controller on simulation experiments.

2. BACKGROUND

2.1 *Induction Motor Model*

We consider the following standard state-space model of the induction motor (Krause et al., 1986),

$$\begin{aligned}
\frac{di_{qs}}{dt} &= \frac{R_r}{L_r L_s \sigma}\lambda_{qs} - \frac{n}{\sigma L_s}\omega_r \lambda_{ds} - \beta i_{qs} + n\omega_r i_{ds} + \frac{1}{\sigma L_s}V_q \\
\frac{di_{ds}}{dt} &= \frac{R_r}{L_r L_s \sigma}\lambda_{ds} + \frac{n}{\sigma L_s}\omega_r \lambda_{qs} - \beta i_{ds} - n\omega_r i_{qs} + \frac{1}{\sigma L_s}V_d \\
\frac{d\lambda_{qs}}{dt} &= -R_s i_{qs} + V_q \\
\frac{d\lambda_{ds}}{dt} &= -R_s i_{ds} + V_d \\
\frac{d\omega_r}{dt} &= \tau_e - B\omega_r - \tau_l,
\end{aligned} \tag{1}$$

in which the state variables, the stator currents i_{qs}, i_{ds}, and fluxes $\lambda_{qs}, \lambda_{ds}$, are set in a reference frame fixed to the stator. Here, $\tau_e = \frac{3}{2}n(i_{qs}\lambda_{ds} - i_{ds}\lambda_{qs})$ denotes the electric torque, with n being the number of pole pairs, τ_l is the load torque, B is the mechanical friction coefficient, and ω_r denotes the rotor speed. The constants σ and β are $\sigma = 1 - M^2/L_s L_r$ and $\beta = R_r/\sigma L_r + R_s/\sigma L_s$, where L_s, L_r, M are the stator, rotor, and mutual inductances, and R_s, R_r the stator and rotor resistances, respectively.

The input voltages V_q and V_d in the model (1) represent the projections of the motor phase voltages V_r, V_s, V_t driving the motor on the so-called q,d-plane, i.e.,

$$\begin{bmatrix} V_q \\ V_d \end{bmatrix} = K \begin{bmatrix} V_r \\ V_s \\ V_t \end{bmatrix}, \quad K = \frac{2}{3}\begin{bmatrix} 1 & -1/2 & -1/2 \\ 0 & -\sqrt{3}/2 & \sqrt{3}/2 \end{bmatrix}. \tag{2}$$

The phase voltages V_r, V_s, V_t are generated by the inverter that drives the motor. Since there are eight admissible combinations of the three pairs of switches of the inverter, the resulting voltage vector driving the motor has eight possible positions (Figure 1). Two of these positions are null vectors, and correspond to the three upper switches closed, V_7, or the three lower switches closed,V_0. The remaining six positions are the active (non null) values of the voltage vector, shown in the q,d-plane in Figure 2.

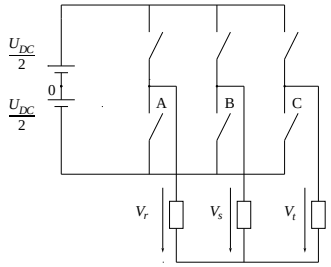

Fig. 1. Inverter scheme.

Since there is usually no neutral connection between the motor and the inverter, the inverter leg voltages V_{A0}, V_{B0}, V_{C0} are not directly applied to the motor phases, but are related to them through the transformation

$$\begin{bmatrix} V_r \\ V_s \\ V_t \end{bmatrix} = \frac{1}{3}\begin{bmatrix} 2 & -1 & -1 \\ -1 & 2 & -1 \\ -1 & -1 & 2 \end{bmatrix}\begin{bmatrix} V_{A0} \\ V_{B0} \\ V_{C0} \end{bmatrix}. \tag{3}$$

Each of these leg voltages can only have two possible values, $\pm\frac{U_{DC}}{2}$, i.e., half of the *DC-bus* U_{DC} (Figure 1).

2.2 *DTFC control*

DTFC is based on limit cycle control (hysteresis loops) of both electric torque and stator flux controlling the output voltage of the inverter. A *switching table* is used to select the best output voltage vector depending on the position of the stator flux and the desired action on electric torque and stator flux (Takahashi and Noguchi, 1986; Depenbrok, 1988). The flux position in the q,d-plane is quantified in six sectors, one for each active voltage vector, $V_k, k = 1,2,\ldots,6$, as shown in Figure 2.

The switching table proposed in Takahashi and Noguchi (1986) is shown in Table 1. Alternative tables exist for specific operation modes, e.g., high/low speed operation, 2/4-quadrant operation, etc. (Buja et al., 1998).

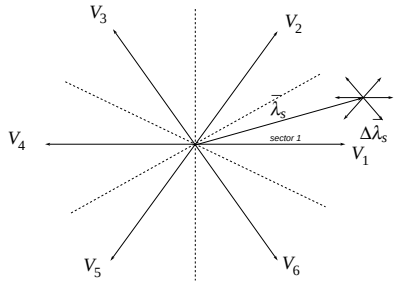

Fig. 2. Active voltage vectors, stator flux vector, and sectors on the q,d-plane.

Desired Effect		Voltage vector depending on sector					
		1	2	3	4	5	6
$\lambda_s\uparrow$	$\tau_e\uparrow$	V_2	V_3	V_4	V_5	V_6	V_1
	τ_e-	V_7	V_0	V_7	V_0	V_7	V_0
	$\tau_e\downarrow$	V_6	V_1	V_2	V_3	V_4	V_5
$\lambda_s\downarrow$	$\tau_e\uparrow$	V_3	V_4	V_5	V_6	V_1	V_2
	τ_e-	V_0	V_7	V_0	V_7	V_0	V_7
	$\tau_e\downarrow$	V_5	V_6	V_1	V_2	V_3	V_4

Table 1. DTFC Table; $x\uparrow$: increase in x, $x\downarrow$: decrease in x, and $x-$: x remains invariant.

3. SLIDING MODE CONTROL

The SMC strategy is based on the design of a discontinuous control signal that drives the system towards special manifolds in the state-space. These manifolds are chosen in a way that the system will have the desired behavior as the state converges to them (e.g., Utkin, 1993; Khalil, 1996).

We now review the basic strategy of SMC for an induction motor, as in Romero and Valla (2000), and show how to compute the inverter DC-bus U_{DC} *off-line* to guarantee the desired performance of the system in steady-state.

3.1 *Basic Strategy*

As in Romero and Valla (2000), we neglect the rotor speed dynamics as compared to the machine electrical dynamics, and consider ω_r in (1) constant for the synthesis process. On writing V_q, V_d in terms of V_{A0}, V_{B0}, V_{C0} using (2) and (3), system (1) may be represented in the form

$$\frac{dx}{dt} = Ax + Bv, \quad \text{where} \quad x = \begin{bmatrix}\lambda_{qs} & \lambda_{ds} & i_{qs} & i_{ds}\end{bmatrix}^T$$

and

$$v = \begin{bmatrix}V_{A0} & V_{B0} & V_{C0}\end{bmatrix}^T. \tag{4}$$

We postulate the SMC manifolds

$$S \doteq \begin{bmatrix}S_1(x)\\ S_2(x)\\ S_3(v)\end{bmatrix} = \begin{bmatrix}(\lambda_{qs}^2+\lambda_{ds}^2)/\lambda_{\text{ref}}^2 - 1\\ \frac{3}{2}n(i_{qs}\lambda_{ds} - i_{ds}\lambda_{qs})/\tau_{\text{ref}} - 1\\ \int (V_{A0}(t)+V_{B0}(t)+V_{C0}(t))dt\end{bmatrix} = 0,$$

where λ_{ref} and τ_{ref} are the references for the flux magnitude and the torque. The manifold $S_1(x)=0$ represents the tracking of the flux magnitude, the manifold $S_2(x)=0$ represents the torque regulation, and the manifold $S_3(v)=0$ represents a voltage balance condition for the inverter.

In Romero and Valla (2000) the candidate Lyapunov function $W = \frac{1}{2}S^TS \geq 0$ is proposed to achieve convergence to the manifolds $S=0$. The time derivative of W along the system trajectories can be written as

$$\frac{dW}{dt} = S^T\frac{dS}{dt} = S^T(H+Dv), \tag{5}$$

where

$$H \doteq \frac{\partial S}{\partial x}Ax + \begin{bmatrix}\frac{\partial S_1}{\partial t}\\ \frac{\partial S_2}{\partial t}\\ 0\end{bmatrix} \text{ and } D \doteq \frac{\partial S}{\partial x}B + \begin{bmatrix}0_{2\times 3}\\ \frac{\partial S_3}{\partial t}\end{bmatrix}. \tag{6}$$

To guarantee the convergence of the system states to the manifolds $S=0$, an appropriate discontinuous control signal is chosen to make $dW/dt < 0$. Because the inverter produces the three independent voltages V_{A0}, V_{B0}, V_{C0}, each of which, in turn, can only take the values $\pm U_{DC}/2$, it is natural to propose the discontinuous control signal v from (4) as

$$v = -U_0\,\text{sign}(S^*), \quad \text{with} \quad S^* \doteq D^TS. \tag{7}$$

Now, on replacing (7) in (5) and rearranging terms, U_0 appears as the design parameter in

$$\begin{aligned}\frac{dW}{dt} &= S^TDD^{-1}H - S^TDU_0\,\text{sign}(S^*)\\ &= (S^*)^TH^* - U_0|S^*|,\end{aligned} \tag{8}$$

where $H^{*T} \doteq (D^{-1}H)^T = [h_1^*\ h_2^*\ h_3^*]$ and $|S^*| = |S_1^*| + |S_2^*| + |S_3^*|$. Hence, from (8), by selecting U_0 such that

$$U_0 > |h_i^*|, \quad \forall i = 1,2,3, \tag{9}$$

convergence to the manifolds $S=0$ is guaranteed (Utkin, 1993).

3.2 *DC-Bus Design*

Note that Equation (9), where h_i^* is a *time-varying function*, needs to be satisfied by appropriately selecting U_0, which is produced by the *constant* DC-bus $U_{DC}/2$. Hence, we propose to select U_0 as the worst-case value under steady-state conditions. To this purpose, we now determine a steady-state expression of $H^* = D^{-1}H$.

Let the reference values λ_{ref} and τ_{ref} be constant. By neglecting ripple, the fluxes and currents in (1) may be assumed as sinusoidal with phases, say $\theta(t)$ and $\theta(t)+\delta$ respectively, with $\delta = cte$. Under these hypotheses, $H = [h_1\ h_2\ h_3]^T$ in (6) turns out to be a constant vector given by

$$
\begin{aligned}
h_1 &= -2R_r(i_{ds}\lambda_{ds}+i_{qs}\lambda_{qs})/\lambda_{\text{ref}} \\
&= -\frac{2R_r}{\lambda_{\text{ref}}}(i_{\max}\lambda_{\max}\cos\delta) \\
&\le -2R_r i_{\max}\lambda_{\max}/\lambda_{\text{ref}} \doteq \bar{h}_1, \\
h_2 &= \beta(i_{qs}\lambda_{ds}-i_{ds}\lambda_{qs})+n\omega_r(i_{ds}\lambda_{ds}+i_{qs}\lambda_{qs}) \\
&\quad -\frac{n\omega_r}{\sigma L_s}(\lambda_{ds}^2+\lambda_{qs}^2) \\
&\le \frac{2\beta}{3n}\tau_{\text{ref}}+n\omega_r i_{\max}\lambda_{\max}-\frac{n\omega_r}{\sigma L_s}\lambda_{\text{ref}}^2 \doteq \bar{h}_2, \\
h_3 &= 0.
\end{aligned}
$$

Where $\bar{H}=[\bar{h}_1\ \bar{h}_2\ 0]^T$ is an upper bound of H. On the other hand D in (6) can be shown to be

$$D=\Lambda * K \tag{10}$$

where K is given in (2), and

$$
\Lambda=\begin{bmatrix}
2\lambda_{qs} & -2\lambda_{ds} & 0 \\
-\frac{3n}{2\sigma L_s}[\sigma L_s i_{ds}-\lambda_{ds}] & -\frac{3n}{2\sigma L_s}[\sigma L_s i_{qs}-\lambda_{qs}] & 0 \\
0 & 0 & 2
\end{bmatrix}.
$$

Because $\sigma L_s i_{ds}$ represents a leakage flux, it can be neglected as compared to λ_{ds}, and the same holds for $\sigma L_s i_{qs}$ with respect to λ_{qs}. Then, it is easy to see that the matrix Λ essentially performs a rotation, i.e., a change of coordinates from a fixed (q,d)-frame to a $(q,d)^{\omega}$-frame rotating at the synchronous frequency $\omega=d\theta/dt$. Then *the matrix $D=\Lambda*K$ transforms the three phase magnitudes in the (R,S,T) frame, to a rotating frame oriented with $\lambda_s=[\lambda_{qs}\ \lambda_{ds}]^T$*. Notice that D is an orthogonal matrix, i.e., $D^T=D^{-1}$.

In summary, under steady-state conditions, the components of $D^{-1}H$ are, essentially, three identical sinusoids shifted $2/3\pi$ rad each. We can then select $U_{DC}=2U_0$ from

$$U_0=\max_t \|D^{-1}\bar{H}\|_{\infty}, \tag{11}$$

which may be easily computed *off-line*.

4. IMPLEMENTATIONS FOR TORQUE RIPPLE REDUCTION

This section presents the main contributions of the paper, namely, two techniques to implement the *on-line* computation of the control signal to achieve reduction of the steady-state torque ripple.

4.1 *Lyapunov-Based Softening of the Control Action*

The proposed constant value of U_0 in (11) has been shown to guarantee, in steady-state, the Lyapunov condition $dW/dt<0$ required by SMC. However, notice from (8) that when $(S^*)^TH^*<0$, this condition would still be guaranteed with $U_0=0$. This observation suggests the possibility of making the control voltage v a null voltage vector, V_0 or V_7, in that case, i.e.,

$$v=\begin{cases} -U_0\,\text{sign}(S^*) & \text{if } (S^*)^TH^*\ge 0, \\ V_0, V_7 & \text{otherwise.} \end{cases} \tag{12}$$

Such a design for the output of inverter requires the *on-line* computation of the value $(S^*)^TH^*=SH$. This computation, however, is not exceedingly complex and produces a significant reduction of torque ripple with respect to the basic SMC strategy of §3 or other conventional DTFC strategies. We further discuss and illustrate this point with simulations in §5.2.

4.2 *Periodic Intersample Modulation by Averaging*

When the control voltage v in (12) does need to be an active voltage vector, $V_k, k=1,\ldots,6$, the proposed SMC strategy applies the full U_0, which we have designed in §3.2 as a worst-case value to satisfy (9) under steady-state conditions. This worst-case value turns out to be particularly conservative at low frequencies, producing a growth of torque ripple.

Since the implementation of the controller is in discrete time, $t=NT_s, N=0,1,2,\ldots$, with a control update time T_s, we propose to perform a *periodic modulation* of the applied voltage vector during the intersample period $[NT_s,(N+1)T_s)$ to further reduce the torque ripple when U_0 is too large. This modulation consists in applying the computed active voltage vector only on the first fraction of the intersample period $[NT_s,NT_s+T_{av})$, while assigning a null voltage vector V_0 or V_7 for the rest of the period $[NT_s+T_{av},(N+1)T_s)$. The time T_{av}, which varies at each sampling time, is computed following an *averaging procedure* similar to that proposed in J.Kang and Sul (1998), as we see next.

We start by computing a virtual "necessary" voltage vector, say U_{0n}, to satisfy (9). At the sampling time $t=NT_s$, the value U_{0n} is obtained computing the "necessary" column voltages as

$$\left[U_{0nA}(NT_s)\ U_{0nB}(NT_s)\ U_{0nC}(NT_s)\right]^T=H^*(NT_s). \tag{13}$$

Then, from (13) we obtain the magnitude of the voltage vector as (for simplicity we omit the argument (NT_s))

$$\|U_{0n}\|_2=\sqrt{U_{0nq}^2+U_{0nd}^2}, \qquad \text{with}$$

where

$$
\begin{aligned}
U_{0nq} &= \frac{2}{3}(U_{0nA}-U_{0nB}/2-U_{0nC}/2), \\
U_{0nd} &= \frac{\sqrt{3}}{3}(U_{0nC}-U_{0nB}).
\end{aligned}
$$

The implementation of U_{0n} is carried out by "averaging" active and null vectors, which may be represented by the expression

$$U_{0n}=\frac{T_{av}V_k+(T_s-T_{av})V_0(V_7)}{T_s},$$

where T_{av} is defined as

$$T_{av} = \frac{3\|U_{0n}\|_2}{2U_{DC}} T_s.$$

The active vector $V_k, k = 1,2,\ldots,6$ is provided by the control law (7), and the selection of the null vector V_0 or V_7 depends on the applied active vector in order to produce the least number of switch commutations. The quantity $\frac{2}{3}U_{DC}$ is the maximum magnitude of the voltage vector when an active vector is applied during the complete intersample interval $[NT_s,(N+1)T_s)$.

In summary, the proposed modulated control law v is given by

$$v(t) = \begin{cases} -U_0 \operatorname{sign}(S^*) & \text{if } SH \geq 0 \; NT_s \leq t < NT_s + T_{av}), \\ V_0, V_7 & \text{otherwise,} \end{cases}$$
$$\text{for } t \in [NT_s,(N+1)T_s). \quad (14)$$

5. DISCUSSION AND SIMULATION RESULTS

This section discusses the performance of the proposed controls (12) and (14), showing their advantages with respect to the basic scheme of §3.1 and conventional DTFC. The evaluation is performed through simulations. The emulated set-up considers a power IGBT inverter with a DC-bus of 500 V. Since the control imposes a variable frequency operation, the speed limit of the converter is fixed by the minimum pulsewidth, which is set at $t_{\min} = 5 \times 10^{-6}$ s. The sampling time is $T_s = 10^{-4}$ s. The motor parameters are given in Table 2.

$R_s = 7\Omega$	$M = 0.1094$Hy
$R_r = 6.4\,\Omega$	$J = 0.0195$Nm/s^2
$L_s = L_r = 0.1289$Hy	$B = 0.002$
$Pn = 1.5$ HP	$n = 2$

Table 2. Motor parameters for simulations.

The simulation results illustrate the performance on

- Machine magnetization,
- Steady-state torque ripple

5.1 *Machine Magnetization*

The proposed control scheme (14) permits the machine magnetization without a torque reference signal, a feature that is not possible with a conventional DTFC scheme. This feature is possible because the proposed scheme can use all eight voltage vectors instead of the five admissible in conventional DTFC. The best choice for machine magnetization is the voltage vector which is collinear to the flux vector in each sector, namely, if the flux vector is in sector k, the best choice is V_k. This situation is not contemplated in conventional DTFC. Figure 3 shows the response of the proposed SMC scheme at start up. Because the proposed control law is not defined at the origin, however, it does require non zero initial conditions for start-up, which were set in $[\lambda_{qs}\ \lambda_{ds}] = [10^{-5}\ 0]$, i.e., the flux vector is in sector $k = 1$, and vector V_1 is selected to magnetize the machine.

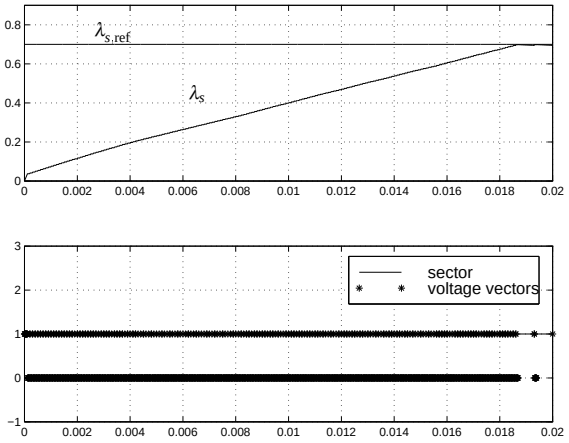

Fig. 3. Reference and flux module at start up.

5.2 *Torque Ripple*

By implementation of the softening of the control action of § 4.1 and the periodic modulation of § 4.2, the proposed control scheme achieves significant reduction of the steady-state torque ripple, as compared with the basic SMC and conventional DTFC schemes.

The ripple phenomenon in DTFC is mainly generated by two factors: (i) conventional DTFC assigns, for a specific action, a single voltage vector for the whole sector and during the whole sampling period, and (ii) voltage vectors producing torque decrease have a stronger action than those producing torque increase.

The assignment of voltage vector to a whole sector in DTFC amounts to computing the control action on an error measurement that is *quantized by sectors*. This quantization by sectors may produce undesirable effects depending on whether the flux vector is at the beginning, in the middle, or at the end of the sector (Bertoluzzo et al., 1999). The proposed SMC takes into account the flux position. Indeed, we can see from the expression of the control signal (7) that the information contained in $S^* = D^T S$ is the flux and torque error per phase, explicitely parameterized by the position of the stator flux vector.

The asymmetrical effect of voltage vectors in torque decrease or increase is discussed in Casadei et al. (1997). Basically, any torque increase $\Delta\tau_e = \tau_e(t_{N+1}) - \tau_e(t_N)$ has always a negative contribution (independently of the voltage input), a situation that becomes worse as speed and load torque go up.

In the proposed SMC strategy (14), the quantity $S^*H^* = SH < 0$ contains the information about when it is necessary to decrement the torque in $S_2 > 0$.

In that case, a null vector V_0, (V_7) is selected as a control action, which results in an important decrease of torque ripple. Since H includes information about the references and their derivatives, a torque inversion, if required, is performed using active vectors, which makes the proposed control scheme suitable for four-quadrant operation. This operation makes our strategy better than those cited in Buja et al. (1998) as State Table A and B, which propose null vectors to decrement flux and torque (in case of torque inversion, these strategies will just apply null vectors, so that the motor will reverse the torque only with its unforced dynamics). Figure 4 shows the torque ripple in the conventional DTFC (top) and the proposed SMC scheme (bottom) at $\omega_r = 148 rad/seg$ and $\tau_l = 7.6 Nm$. The torque ripple produced by the proposed strategy is about half that of conventional DTFC.

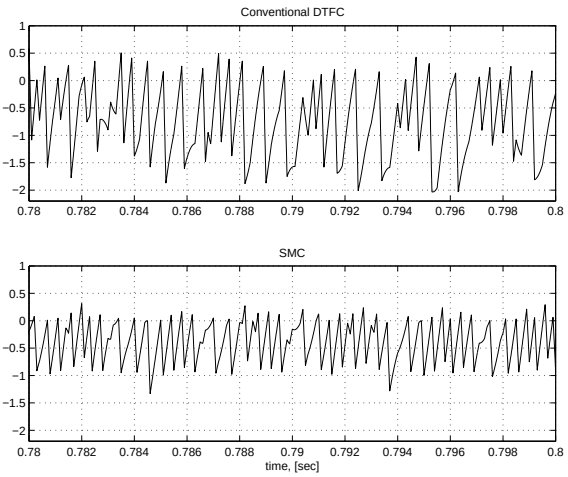

Fig. 4. Torque ripple: conventional DTFC vs. SMC.

Figure 5 shows (from top to bottom) the Conventional DTFC strategy, the SMC strategy without intersampling and the benefits of the application of the *periodic intersampling modulation technique*, developed in § 4.2 at low speed. This figure emulates the situation where the application of the total DC-bus, calculated in § 3.2 results too big for this operational condition. The simulation conditions where set to $\omega_r = 9 rad/seg$ and $\tau_l = 7.6 Nm$.

6. CONCLUSIONS

We have presented a DTFC strategy using the SMC approach implementation for torque ripple reduction, namely, the use of null vectors to correct special error conditions, and a periodic modulation tecnique to apply the correct magnitud of the control signal. This methodology presents substantial advantages over conventional DTFC, namely, the possibility of machine magnetization without a torque reference signal, more control degrees of freedom, and use of (non quantized) flux space vector information in the control computation.

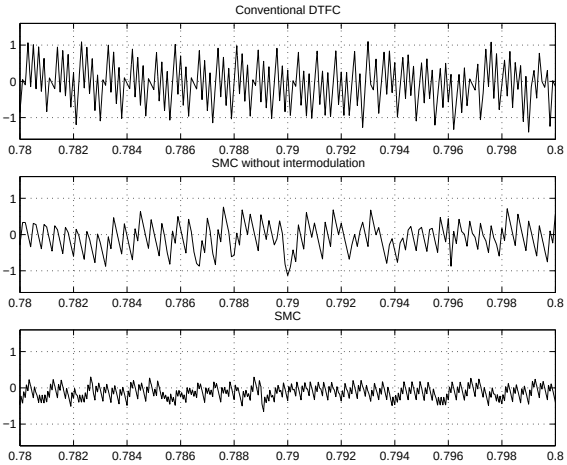

Fig. 5. Intersampling modulation effect at low speed

References

M. Bertoluzzo, G. Buja, and R. Menis. Analytical formulation of the direct control of induction motor drives. In *IEEE-Int. Symp. Industrial Electronics*, pages Ps14–Ps20, Bled, Slovenia, 1999.

G. Buja, D. Casadei, and G. Serra. Direct stator flux and torque control of an induction motor: theorethical analysis and experimental results. In *IEEE Proc. Industrial Electronic Conf.*, pages T50–T64, Aachen, Germany, 1998.

D. Casadei, G. Serra, and A. Tani. Analitical investigation of torque and flux ripple in dtc scheme for induction motors. In *IEEE Proc. of Industrial Electronic Conf., IECON'97*, pages 552–556, New Orleans, USA, 1997.

M. Depenbrok. Direct Self-Control (DSC) of Inverter-Fed Induction Machine. *IEEE Trans. on Power Electronics.*, 3:420–429, 1988.

N. Idris and A. Yatim. Reduced torque ripple and constant switching frequency strategy for direct torque control of induction machine. In *IEEE Appl. Power Electronics Conf.*, pages 154–160, New Orleans, USA, 2000.

J.Kang and S. Sul. Torque ripple minimization strategy for direct torque control of induction motor. In 33^{rd} *Annual Meeting Industrial Applications Soc., IEEE-IAS'98, Oct. 98*, pages 546–551, St. Louis, USA, 1998.

M. Kazmierkowki and A. Kasprowicz. Improve Direct Torque and Flux Vector Control of PWM Inverter-Fed Induction Drives. *IEEE Trans. Industrial Electronics.*, 42:344–349, 1995.

H. K. Khalil. *Nonlinear systems*. Prentice-Hall, 2nd edition, 1996.

P. Krause, O. Wasynnczuc, and S. Sudhoff. *Analysis of Electric Machinery*. McGraw-Hill, 1986.

Hoang Le-Huy. Comparison of field oriented control and direct torque control for induction motor drives. *No se*, 44:35–46, 1995.

M. Romero and M.I. Valla. DTFC of induction motor with sliding-mode approach. In *IEEE Int. Symp. Industrial Electronics*, pages 1287–1297, Cholula, Mexico, 2000.

I. Takahashi and T. Noguchi. A New Quick response and High - Efficiency Control Strategy of an Induction Motor. *IEEE Trans. Industry Appl.*, 22:820–827, 1986.

I. Takahashi and T. Noguchi. Take a look back upon the past decade of direct torque control. In *IEEE Proc. of Industrial Electronic Conf.*, pages 546–551, New Orleans, USA, 1997.

Vadim Utkin. Sliding mode control design principles and application to electrical drives. *IEEE Trans. Ind. Electron.*, 40:23–36, 1993.

Peter Vas. *Sensorless Vector Control and Direct Torque Control*. Oxford University Press, 1998.

Z. Yan, C. Jin, and V. Utkin. Sensorless Sliding-Mode Control of Induction Motors. *IEEE Trans. Ind. Electron.*, 47:1287–1297, 2000.